OPEN

Relationship Between Radiomics and Risk of Lymph Node Metastasis in Pancreatic Ductal Adenocarcinoma

Yun Bian, MD, PhD, Shiwei Guo, MD, PhD,† Hui Jiang, MD, PhD,‡ Suizhi Gao, MMS,† Chenwei Shao, MD, PhD,* Kai Cao, MD, PhD,* Xu Fang, MMS,* Jing Li, MD, PhD,* Li Wang, MD, PhD,* Wenda Hua, MMS,§ Jianming Zheng, MD, PhD,‡ Gang Jin, MD, PhD,† and Jianping Lu, MD, PhD**

Objective: The objective of this study was to explore the exact relationship between the arterial radiomics score (rad-score) and lymph node (LN) metastasis in pancreatic ductal adenocarcinoma (PDAC).

Methods: A total of 225 patients with pathologically confirmed PDAC who underwent multislice computed tomography within 1 month of resection from December 2016 to August 2017 were retrospectively studied. For each patient, 1029 radiomics features of arterial phase were extracted, which were reduced using the least absolute shrinkage and selection operator logistic regression algorithm. Multivariate logistic regression models were used to analyze the association between the arterial rad-score and LN metastasis.

Results: Lymph node–negative and LN-positive patients accounted for 107 (47.56%) and 118 (52.44%) of the cohort, respectively. The rad-score, which consisted of 12 selected features of the arterial phase, was significantly associated with LN status ($P < 0.05$). Univariate analysis revealed that the arterial rad-score and T stage were independently and positively associated with risk of LN metastasis ($P < 0.05$). Multivariate analyses revealed a significant association between the arterial rad-score and the LN metastasis ($P < 0.0001$). Higher arterial rad-score was associated with LN metastasis (P for trend <0.0001).

Conclusions: The arterial rad-score is independently and positively associated with the risk of LN metastasis in PDAC.

Key Words: pancreatic neoplasm, carcinoma, pancreatic ductal adenocarcinoma, lymph nodes, computed tomography, radiomics

(*Pancreas* 2019;48: 1195–1203)

Pancreatic cancer is highly lethal with a mortality rate that closely parallels its incidence.[1,2] Surgical resection is regarded as the only potentially curative treatment that can result in significantly longer survival periods compared with other treatment options. Unfortunately, not all patients with pancreatic ductal adenocarcinoma (PDAC) can benefit from the pancreatic radical surgery owing to the peculiar features of this tumor that is already lymph node (LN) metastatic at the time of diagnosis. The LN metastasis is observed in more than 70% of resected ductal adenocarcinomas and is present even when the primary tumor is smaller than 2 cm in size.[3] The LN variables constitute one of the most important sole predictors of survival, which can be accurately evaluated via postoperative pathological examination. However, preoperative prediction of the nodal status is difficult, even with the most sophisticated radiological techniques.[4]

Endoscopic ultrasonography–guided fine-needle aspiration (EUS-FNA) is considered a fairly sensitive tool for distinguishing the LN metastasis from the pancreatic lesions. However, EUS-FNA is an invasive diagnostic tool that is expensive and time-consuming with a significant risk of complications.[5,6] Magnetic resonance imaging also has several limiting factors for determining the LN status in clinical settings, including spatial resolution problems, motion artifacts, and dose-dependent oversaturation artifacts.[7] Multislice computed tomography (MSCT) is the best initial diagnostic test for pancreatic cancer. However, a meta-analysis that investigated efficacy of computed tomography (CT) for assessing the extraregional LN metastasis in pancreatic and periampullary cancers yielded a pooled sensitivity of 25% and a positive predictive value of 28%.[8] The important clinical objectives, including differentiation of reactive, inflammatory lymphadenopathy from malignant lymphadenopathy and detection/visualization of the metastatic LNs could not be achieved by this technique.

Radiomics is an emerging field that involves conversion of imaging data into a high-dimensional mineable feature space using a large number of automatically extracted data-characterization algorithms.[9,10] It provides a noninvasive method for LN metastasis prediction.[11–15] However, only a few studies have focused on the association between radiomics and the LN metastasis in PDAC.

Thus, the primary objective of our study was to evaluate whether the arterial radiomics score (rad-score) of PDAC was associated with LN metastasis on preoperative MSCT.

From the *Department of Radiology, †Department of Pancreatic Surgery, and ‡Department of Pathology, Changhai Hospital, The Navy Military Medical University, Shanghai; and §Huiying Medical Technology (Beijing) Co, Ltd, Beijing, China.

Received for publication February 21, 2019; accepted August 14, 2019.

Address correspondence to: Jianping Lu, MD, PhD, Department of Radiology, Changhai Hospital, The Navy Military Medical University, 168 Changhai Rd, Shanghai 200433, China (e-mail: cjr.lujianping@vip.163.com). Gang Jin, MD, PhD, Department of Pancreatic Surgery, Changhai Hospital, The Navy Military Medical University, 168 Changhai Rd, Shanghai 200433, China (e-mail: jingang@sohu.com).

This work was supported by National Science Foundation for Scientists of China (81871352), National Science Foundation for Young Scientists of China (81701689, 81601468), the 63-class General Financial Grant from the China Postdoctoral Science Foundation (2018M633714), Key Junior College of National Clinical of China, Shanghai Technology Innovation Project 2017 on Clinical Medicine (17411952200), Project of Precision Medical Transformation Application of NMMU (2017JZ42), and Top Project of the Military Medical Science and Technology Youth Training Program (17QNP017).

The authors declare no conflict of interest.

L.W. and S.G. conceptualized the study. G.J., J.L. designed the statistical model. Y.B., S.G., C.M., X.F., J.L., K.C., W.H., performed the experiments and data analysis. H.J. and J.Z. provided the pathological data and carried out image analysis. Y.B. wrote the first draft of the manuscript. All authors contributed to critical review of the manuscript.

This study was reviewed and approved by the Biomedical Research Ethics Committee of the Naval Military Medical University of the Chinese People's Liberation Army. The relevant provisions and principles of human biomedical ethics were maintained. All patients signed an informed consent form before the examination.

Supplemental digital contents are available for this article. Direct URL citations appear in the printed text and are provided in the HTML and PDF versions of this article on the journal's Web site (www.pancreasjournal.com).

DOI: 10.1097/MPA.0000000000001404

MATERIALS AND METHODS

Patients

This retrospective single-center study was reviewed and approved by the Biomedical Research Ethics Committee of the Navy Military Medical University of the Chinese People's Liberation Army. Patients were excluded from the study cohort if one of the following criteria was met: patients who did not have a preoperative standard contrast-enhanced MSCT, did not have enhanced MSCT within a month before surgery, had received any treatment (radiotherapy, chemotherapy, or chemoradiotherapy) before their imaging studies were performed, had not undergone surgical treatment, were not diagnosed with PDAC by both hematoxylin and eosin staining and immunohistochemistry, had pathologically confirmed PDAC with mixed differentiation, had pancreatic lesions that could not be visualized in MSCT images, had other tumors in the pancreas, or did not have preoperative serum carbohydrate antigen (CA) 19-9 concentration, were excluded from the study. Consequently, a total of 225 consecutive patients with PDAC, 137 males (mean age, 60.02 years; age range, 31–77 years) and 88 females (mean age, 63.28 years; age range, 32–80 years), were included in this cross-sectional study at our institution. Data were gathered from records January 2014 to December 2017. A flowchart of the study population is presented in Figure 1.

CT Scanning

A 640-slice CT scanner (Aquilion ONE, Canon Medical Systems, Tokyo, Japan) was used. The CT scan parameters were as follows: 120 kV, 150 effective mAs, beam collimation of 100 × 0.5 mm, a matrix of 350 × 350, and a gantry rotation time of 0.5 seconds. After performing a nonenhanced CT, a dynamic contrast-enhanced CT scan was performed. The scan delayed time was determined according to the test bolus. The contrast agent, 90 to 95 mL of 355 mgI/mL iopromide (Ultravist 370, Bayer Schering Pharma, Berlin, Germany), was injected at a rate of 5.5 mL/s using a high-pressure syringe via the forearm vein followed by 98 mL of normal saline to flush the tube. The contrast-enhanced CT scan was performed in arterial (20–25 seconds), portal venous (60–70 seconds), and delayed (110–130 seconds) phases after the contrast agent injection. The scanning range extended from the level of the diaphragm to the level of the pelvis.

Radiomics Workflow

The radiomics workflow included (*a*) image segmentation, (*b*) feature extraction, and (*c*) feature reduction and selection (Fig. 2).

Image Segmentation, Radiomics Feature Extraction, and Radiomics Signature Building

In this study, the original cross-sectional arterial images were used for subsequent analysis. The draw tool available in the Editor module of the 3D Slicer (version 3.3.3; Boston, Mass) (open source software, https://www.slicer.org/) was used to delineate the tumors in multiple slices. In this study, the volume of interest was extracted by stacking the corresponding regions of interest delineated slice-by-slice for each patient.

Radiomics feature extraction was conducted using an open source Python package, Pyradiomics 1.2.0 (http://www.radiomics.io/pyradiomics.html).[16] The feature extraction methods used in this study included 2 categories: original feature classes

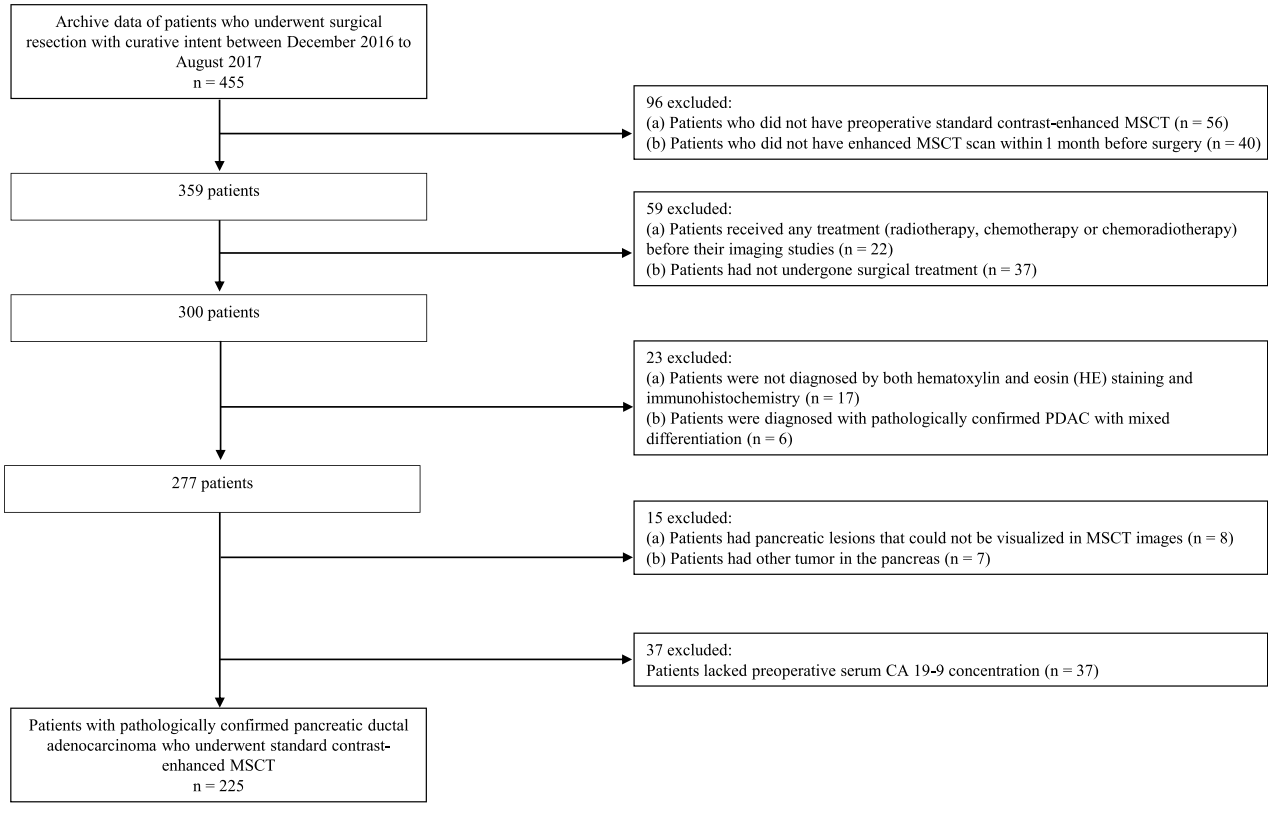

FIGURE 1. The patient enrolment process for this study.

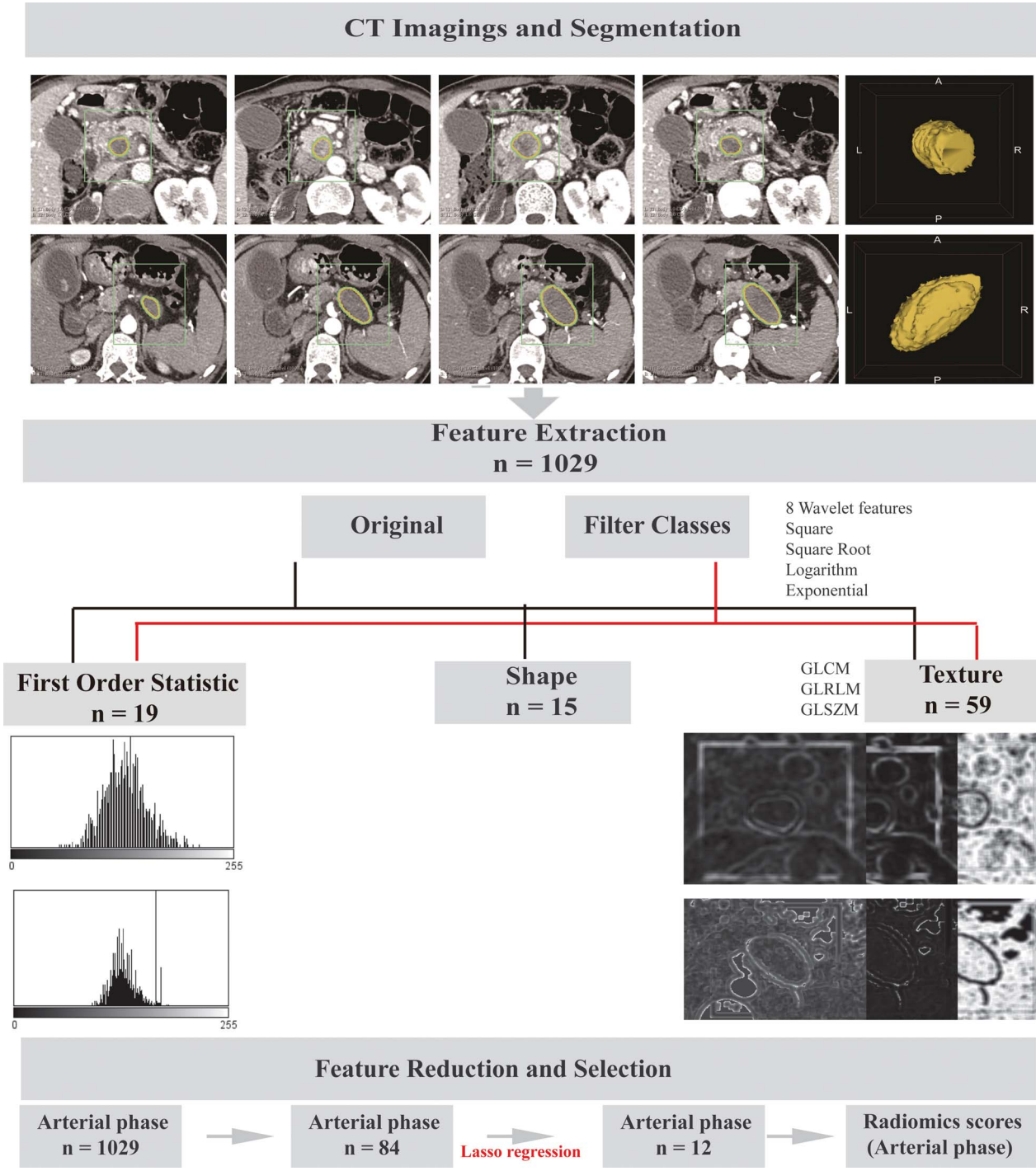

FIGURE 2. Radiomics workflow.

and filter classes. The filter classes further included 5 categories: wavelet, square, square root, logarithm, and exponential. A total of 1029 2-dimensional and 3-dimensional features from primary tumors in arterial phase were extracted and divided into 5 groups: (*a*) first-order statistics, (*b*) shape features, (*c*) gray-level cooccurrence matrix features, (*d*) gray-level size zone matrix features, and (*e*) gray-level run-length matrix features. More information about the procedures for image segmentation and radiomics feature extraction is reported in Supplemental Digital Content 1 (http://links.lww.com/MPA/A740).

To assess interobserver reliability, the region of interest segmentation was performed in a blinded fashion by 2 radiologists, reader 1 (L.W., with 30 years of experience in imaging) and reader 2 (X.F., with 5 years of experience in imaging). Both were aware of PDAC diagnosis but were blinded to the clinical and pathologic details. To evaluate intraobserver reliability, reader 1 repeated the

feature extraction twice in a 1-week period. Reader 1 completed the remaining image segmentations, and the readout sessions were conducted over a period of 1 month. The reliability was calculated by using intraclass correlation coefficient. Radiomic features with both intraobserver and interobserver intraclass correlation coefficient values greater than 0.75 (indicating excellent stability) were selected for subsequent investigation (Supplemental Digital Content 2, http://links.lww.com/MPA/A740).

Because the radiomics features were very high-dimensional compared with the sample size, the feature selection consisted of 3 steps. First, variance analysis was performed, and features with low variance among the groups were removed. Second, Pearson correlation analysis was performed, and features with no significant correlation between radiomics features and the LN metastasis were removed. Finally, the least absolute shrinkage and selection operator (LASSO) logistic regression algorithm, suitable for performing regression analysis of high-dimensional data, was used to select the most useful associated features.[17] The LASSO logistic regression model was used with a penalty parameter tuning that was conducted by a 10-fold cross-validation based on minimum criteria. A rad-score was calculated for each patient via a linear combination of selected features that were weighted by their respective coefficients. More information about the feature selection can be found in Supplemental Digital Content 3 (http://links.lww.com/MPA/A740).

Pathological Image Analysis

All the specimens were analyzed by a specialized pathologist. Pathological examination and analysis were standardized according to a formal protocol.[3] The resected specimens were immediately fixed in formalin for 24 hours. Subsequently, they were cut horizontally into 5-mm tissue blocks that were dehydrated and embedded in paraffin. Finally, 5-μm large sections were stained with hematoxylin and eosin for conventional histology. Each large section was carefully examined by light microscopy. Tumor-node-metastasis staging was performed on the basis of the *American Joint Committee on Cancer TNM Staging Manual, Eighth Edition*.[18]

Statistical Analyses

Normal distribution and variance homogeneity tests were performed on all continuous variables. Continuous variables with a normal distribution were expressed as mean and standard deviation; otherwise, they were expressed in terms of median and interquartile range. The arterial rad-score was expressed as 10 times. First, we examined group differences in terms of age, sex, body mass index (BMI), CA 19-9 level, tumor location, tumor (T) grade, grade of differentiation, and the arterial rad-score between LN-positive and LN-negative patients. Student *t* test (normal distribution), Kruskal-Wallis *H* test (skewed distribution), and χ^2 test (categorical variables) were used to determine the statistical differences between the 2 groups. Second, patients were categorized into quartiles (Q1 < −1.68, Q2 [−1.68 to −0.14], Q3 [−0.14 to 1.33], and Q4 ≥ 1.33) on the basis of the arterial rad-score, with Q1 as the reference group. Univariate regression analysis was applied to estimate the effect size between all variables and the LN metastasis. Third, the subgroup analyses were performed using stratified linear regression models for the all covariables. The following potential-effect modifiers were considered: age (<59, 59–66, ≥66 years), sex, BMI (15.04–21.48, 21.5–23.83, 23.88–32.46 kg/m^2), CA 19-9 level (≤37, >37 μg/L), tumor location, T stage, and grade of differentiation. Lastly, multivariable logistic models were used to evaluate the associations between exposure (the arterial rad-score) and outcome (LN metastasis), and in an age-, sex-, and BMI-adjusted model 2, and further adjusting for CA 19-9-, tumor location-, T stage-, and grade of differentiation–adjusted model 3. *P* values for trend among various arterial rad-score were derived from the generalized linear regression models, assuming equally spaced levels for 4 groups. The interaction of subgroup was inspected by the likelihood ration test.

A 2-tailed *P* value of <0.05 was considered statistically significant. All analyses were performed with SPSS (version 20.0, IBM, Inc, Armonk, NY), R software (version 3.3.3, The R Foundation for Statistical Computing, Vienna, Austria), and EmpowerStats (X&Y Solutions, Inc, Boston, Mass).

RESULTS

Clinical Characteristics

The LN-negative and the LN-positive patients accounted for 47.56% (107) and 52.44% (118) of the study cohort, respectively. There was a significant difference in T stage between the LN-positive and the LN-negative patients. However, there were no

TABLE 1. Baseline Characteristics of Patients With PDAC

Characteristics	LN Negative (n = 107)	LN Positive (n = 118)	*P*
Age, mean (SD), y	62.39 (7.58)	60.31 (9.59)	0.073
BMI, mean (SD), kg/m^2	22.73 (2.84)	22.58 (2.54)	0.667
Sex, n (%)			
Male	63 (58.88)	74 (62.71)	0.556
Female	44 (41.12)	44 (37.29)	
CA 19-9, median (range), μg/L	332.12 (48.45–1134.70)	299.48 (82.39–1200.00)	0.656
Location, n (%)			
Head	60 (56.07)	74 (62.71)	0.31
Body and tail	47 (43.93)	44 (37.29)	
T stage, n (%)			
T1	19 (17.76)	8 (6.78)	0.037
T2	20 (18.69)	28 (23.73)	
T3–4	68 (63.55)	82 (69.49)	
Grade of differentiation, n (%)			
Well to moderately	88 (82.24)	97 (82.20)	1.0
Poorly to undifferentiated	19 (17.76)	21 (17.80)	

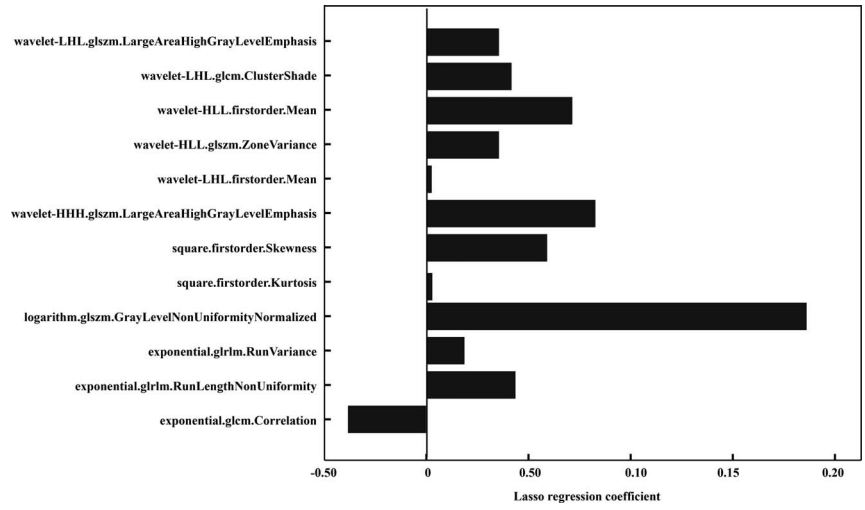

FIGURE 3. Radiomic features selected by LASSO regularization.

significant differences in age, sex, CA 19-9 level, tumor location, or grade of differentiation ($P > 0.05$) between the 2 groups. The patient characteristics are shown in Table 1.

Radiomics Analysis

A total of 1029 radiomics features from the arterial phase of CT were extracted and grouped on the basis of the LN metastasis. However, the radiomics features that were not significantly different between the groups or did not have significant correlations with the LN metastasis were removed. Consequently, 84 radiomics features were selected from the arterial phase that were further reduced using a LASSO logistic regression model. Finally, the radiomics characteristics were reduced to 12 features (Fig. 3). The LASSO logistic regression formula was used to obtain the rad-score for the arterial phase. The rad-score calculation formula is presented in Supplemental Digital Content 3 (http://links.lww.com/MPA/A740). There was a significant difference in rad-scores during the arterial phase between the LN-positive and the LN-negative patients ($P = 0.002$) (Fig. 4).

Univariate Analysis for Each Parameter Variable

The results of univariate analysis are shown in Table 2. They demonstrate that the arterial rad-score ($P < 0.0001$) and the T

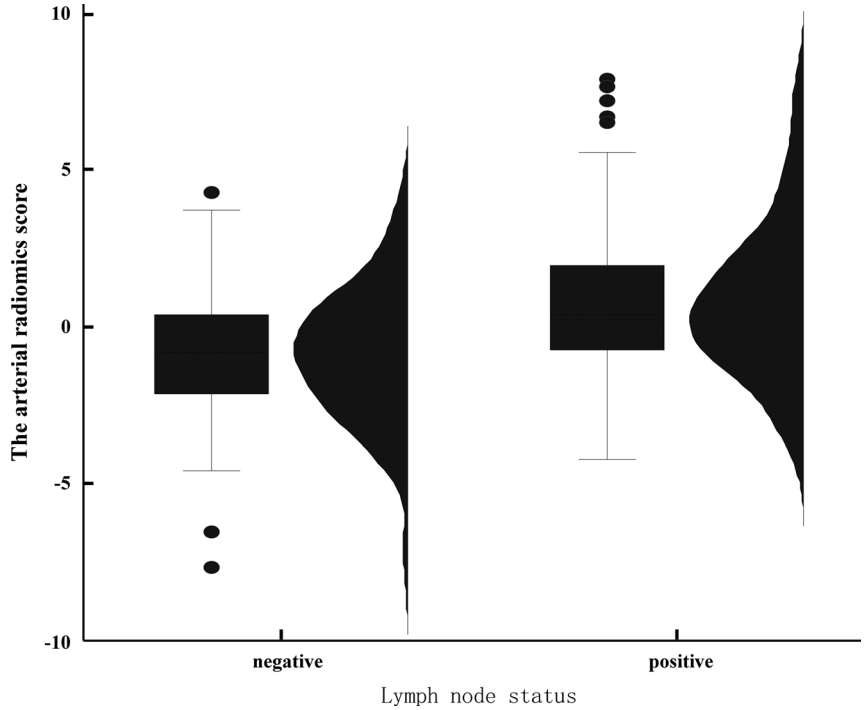

FIGURE 4. Combo chart of rad-scores by the LASSO regression formula among the arterial phases of CT. Combo chart includes both the box plot and the density plot.

TABLE 2. The Result of Univariate Analysis

Variables	Statistics	OR (95% CI)	*P*
Rad-score, median (IQR)	−0.12 (−1.68 to 1.39)	1.42 (1.23–1.63)	<0.0001
Rad-score, n (%)			
Q1	56 (24.89)	1.0 (Reference)	
Q2	56 (24.89)	2.14 (0.98–4.63)	0.05
Q3	56 (24.89)	2.84 (1.31–6.18)	0.01
Q4	57 (25.33)	7.05 (3.07–16.15)	<0.0001
Age, y, n (%)			
<59	73 (32.44)	1.0 (Reference)	
59–66	71 (31.56)	0.61 (0.31–1.17)	0.14
≥66	81 (36.00)	0.75 (0.40–1.42)	0.38
Sex, n (%)			
Male	137 (60.89)	1.0 (Reference)	
Female	88 (39.11)	0.85 (0.50–1.46)	0.56
BMI, kg/m^2, n (%)			
15.04–21.48	75 (33.33)	1.0 (Reference)	
21.5–23.83	74 (32.89)	0.79 (0.41–1.50)	0.46
23.88–32.46	76 (33.78)	0.97 (0.51–1.84)	0.93
CA 19-9, μg/L, n (%)			
≤37	44 (19.56)	1.0 (Reference)	
>37	181 (80.44)	1.26 (0.65–2.45)	0.49
Location, n (%)			
Head	134 (59.56)	1.0 (Reference)	
Body and tail	91 (40.44)	0.76 (0.45–1.29)	0.31
T stage, n (%)			
T1	27 (12.00)	1.0 (Reference)	
T2	48 (21.33)	3.32 (1.22–9.09)	0.02
T3–4	150 (66.67)	2.86 (1.18–6.95)	0.02
Grade of differentiation, n (%)			
Well to moderately	185 (82.22)	1.0 (Reference)	
Poorly to undifferentiated	40 (17.78)	1.00 (0.51–1.99)	0.99

Patients were categorized into quartiles of rad-score (Q1 < −1.68, Q2 [−1.68 to −0.14], Q3 [−0.14 to 1.33], and Q4 ≥ 1.33).
IQR indicates interquartile range.

stage ($P = 0.02$) were significantly associated with an increased risk for the LN metastasis.

Stratified Analysis of LN Metastasis

Stratified analyses revealed that the impact of the arterial rad-score on the LN metastasis was not affected by age, sex, BMI, CA 19-9 level, tumor location, T stage, or grade of differentiation (P for interaction = 0.56, 0.28, 0.95, 0.51, 0.09, 0.76, and 0.99, respectively). The trend of an increasing arterial rad-score with a higher likelihood of LN metastasis among age groups of younger than 59 years and 66 years and older, sex, BMI, CA 19-9 level higher than 37 μg/L, tumor location, T2 to T4 stage, and grade of differentiation (P for trend <0.05). The results of stratified analysis are shown in Table 3.

Multivariate Analyses

In the crude model (model 1), the arterial rad-score correlated with LN metastasis ($P < 0.0001$; odds ratio [OR], 1.42; 95% confidence interval [CI], 1.23–1.63). In the minimally adjusted model (adjusted for age, sex, and BMI; model 2), the effect size also had a significant correlation with LN metastasis ($P < 0.0001$; OR, 1.44; 95% CI, 1.25–1.66). After further adjusting other covariates (fully adjusted, model 3), significant correlation could still be identified ($P < 0.0001$; OR, 1.43; 95% CI, 1.23–1.66). Furthermore, we treated the arterial rad-score as a categorical variable (quartile) for sensitivity analysis and observed the same trend (P for trend <0.0001). The results of multivariate analysis are shown in Table 4.

DISCUSSION

The present study aimed to examine the relationship between the arterial rad-score and LN metastasis among patients with PDAC. As shown by the fully adjusted model (model 3), the arterial rad-score was significantly associated with LN metastasis. High-risk patients had a 1.43-fold increased risk of LN metastasis than that of low-risk patients. Arterial rad-score as a categorical variable (quartile) revealed 2.16-, 2.74-, and 7.43-fold increased risk of LN metastasis in Q2, Q3, and Q4, respectively, compared with that in Q1. Hence, a higher arterial rad-score was associated with a higher risk of LN metastasis (P for trend <0.001).

Pancreatic ductal adenocarcinoma is characterized by an extremely high mortality rate and a poor prognosis, which are largely attributed to the difficulties associated with early diagnosis and limited therapeutic options. The number of positive LNs has been shown as a crucial and independent prognostic factor for an overall

TABLE 3. Effect Size of Rad-score on LN Metastasis in Prespecified and Exploratory Subgroups in Each Subgroup

Outcome	Events, number	OR (95% CI)	Q1	Q2	Q3	Q4	*P* for Trend	*P* for Interaction
Age, y								0.56
<59	73	1.46 (1.13–1.90)*	1.0 (Reference)	2.32 (0.63–8.58)	1.62 (0.41–6.39)	9.75 (2.16–43.98)*	0.004	
59–66	71	1.27 (0.99–1.63)	1.0 (Reference)	1.69 (0.39–7.27)	2.05 (0.48–8.77)	3.75 (0.79–17.72)	0.086	
≥66	81	1.53 (1.21–1.95)*	1.0 (Reference)	2.72 (0.70–10.63)	6.80 (1.77–26.18)*	10.20 (2.46–42.23)*	0.001	
Sex								0.28
Male	137	1.51 (1.25–1.84)*	1.0 (Reference)	5.62 (1.94–16.32)*	3.80 (1.35–10.71)*	11.81 (3.88–35.97)*	<0.0001	
Female	88	1.29 (1.05–1.59)*	1.0 (Reference)	0.55 (0.16–1.89)	1.93 (0.57–6.47)	3.33 (0.93–12.01)	0.024	
BMI, kg/m^2								0.95
15.04–21.48	75	1.45 (1.12–1.88)*	1.0 (Reference)	1.07 (0.29–3.99)	2.50 (0.59–10.62)	7.08 (1.60–31.33)*	0.004	
21.5–23.83	74	1.44 (1.14–1.84)*	1.0 (Reference)	4.08 (0.86–19.37)	3.50 (0.89–13.76)	7.58 (1.74–33.09)*	0.009	
23.88–32.46	76	1.38 (1.09–1.76)*	1.0 (Reference)	2.62 (0.74–9.21)	3.06 (0.82–11.44)	6.96 (1.66–29.26)*	0.007	
CA 19-9, μg/L								0.51
≤37	44	1.29 (0.96–1.73)	1.0 (Reference)	2.33 (0.46–11.81)	1.60 (0.27–9.49)	3.00 (0.52–17.16)	0.264	
>37	181	1.45 (1.23–1.70)*	1.0 (Reference)	2.07 (0.86–5.01)	3.22 (1.35–7.67)*	8.82 (3.40–22.87)*	<0.0001	
Location								0.09
Head	134	1.32 (1.12–1.57)*	1.0 (Reference)	2.14 (0.83–5.53)	2.56 (0.99–6.61)*	4.37 (1.55–12.33)*	0.004	
Body and tail	91	1.75 (1.31–2.33)*	1.0 (Reference)	4.20 (0.77–22.91)	6.42 (1.18–34.86)*	25.67 (4.53–145.50)*	<0.0001	
T stage								0.76
T1	27	1.55 (0.99–2.42)*	1.0 (Reference)	2.75 (0.28–26.61)	5.50 (0.46–65.16)	5.50 (0.46–65.16)	0.121	
T2	48	1.51 (1.03–2.20)*	1.0 (Reference)	3.33 (0.47–23.47)	2.86 (0.42–19.65)	12.50 (1.34–116.80)*	0.031	
T3–4	150	1.35 (1.14–1.59)*	1.0 (Reference)	1.58 (0.62–4.07)	2.32 (0.91–5.95)	5.48 (2.05–14.69)*	0.001	
Grade of differentiation								0.99
Well to moderately	185	1.42 (1.22–1.65)*	1.0 (Reference)	2.54 (1.08–5.96)*	2.76 (1.18–6.43)*	8.50 (3.32–21.73)*	<0.0001	
Poorly to undifferentiated	40	1.42 (0.97–2.06)	1.0 (Reference)	0.95 (0.14–6.28)	3.33 (0.45–24.44)	3.33 (0.51–21.58)	0.122	

Patients were categorized into quartiles of radiomics score (Q1 < −1.68, Q2 [−1.68 to −0.14], Q3 [−0.14 to 1.33], and Q4 ≥ 1.33).

*$P < 0.05$.

TABLE 4. Relationship Between the Arterial Rad-score and LN Metastasis in Different Models

	Model 1		Model 2		Model 3	
Variable	**OR (95% CI)**	***P***	**OR (95% CI)**	***P***	**OR (95% CI)**	***P***
Rad-score	1.42 (1.23–1.63)	<0.0001	1.44 (1.25–1.66)	<0.0001	1.43 (1.23–1.66)	<0.0001
Rad-score						
Q1	1.0 (Reference)		1.0 (reference)		1.0 (Reference)	
Q2	2.14 (0.98–4.63)	0.050	2.31 (1.04–5.11)	0.039	2.16 (0.97–4.84)	0.060
Q3	2.84 (1.31–6.18)	0.008	3.32 (1.49–7.41)	0.003	2.74 (1.22–6.14)	0.014
Q4	7.05 (3.07–16.15)	<0.0001	7.60 (3.26–17.71)	<0.0001	7.43 (3.12–17.72)	<0.0001
P for trend	<0.0001		<0.0001		<0.0001	

Patients were categorized into quartiles of radiomics score (Q1 < −1.68, Q2 [−1.68 to −0.14], Q3 [−0.14 to 1.33], and Q4 ≥ 1.33). Model 1, we did not adjust for other covariants. Model 2, we adjusted for age, sex, and BMI. Model 3, we further adjusted for CA 19-9, location, T stage, and pathologic grade.

survival in PDAC patients.[19] Pancreatectomy is the most effective method to improve the long-term survival of PDAC patients. However, whether or not pancreatectomy should include a standard or an extended lymphadenectomy is still debated.[20,21] Thus, an accurate preoperative LN staging of PDAC is essential for providing patients with an appropriate counsel regarding surgical decisions and prognosis. However, it is difficult to achieve an accurate preoperative LN staging with the currently available methods.

Endoscopic ultrasound–guided fine-needle aspiration is considered a fairly sensitive tool for detection of the pancreatic lesions and offers diagnostic value for both the primary tumor and the LN metastasis.[5,6] It can be used to obtain a piece of tissue that can provide sufficient histological information for the diagnosis of peripancreaticobiliary LN. For FNA of LNs, the amount of tissue acquired is usually adequate, wherein suction is not recommended to reduce blood contamination.[22] In addition, EUS-FNA is affected by various factors, such as the scope position,[23] lesion characteristics, lesion environment, and evaluating pathologist.[23–26] Positron emission tomography/CT may be useful for identification of the most suspicious nodes for biopsy; however, its use is limited for evaluating small-volume diseases and cannot differentiate between inflammatory lymphadenopathy and metastatic lymphadenopathy.[27] Similarly, magnetic resonance imaging has several limiting factors associated with determination of LN status in clinical settings, namely, spatial resolution problems, motion artifacts, and dose-dependent oversaturation artifacts.[7] Thus, the most widely used preoperative staging modality for pancreatic cancer is CT.[28,29] Computed tomography can accurately assess tumor size and vessel involvement; however, its diagnostic accuracy is low owing to poor sensitivity.[8] An LN diameter of more than 10 mm is considered as the criterion for LN metastasis in many studies; however, it has poor sensitivity (20%–38%) .[30–33] The criteria for metastatic LNs also include nonuniform density, nonuniform enhancement, internal necrosis, LN fusion, ill-defined borders, or involvement of the surrounding organs or blood vessels.[18,34] However, the abovementioned diagnostic criteria also yield low diagnostic accuracy and sensitivity.

There are several main limitations of the preoperative imaging studies of LNs. First, it is difficult to establish one-to-one correlation between the LN imaging findings and the pathological evidence of LN metastasis. Second, CT provides limited visualization to identify metastatic LNs. Finally, there is no significant correlation between the LN metastasis, and the clinical and pathologic characteristics of PDAC patients. In addition, local inflammation secondary to malignant biliary obstruction may independently result in enlarged LNs.[35] In the current study, we found that there was no significant correlation between the LN metastasis and age, sex, BMI, CA 19-9 level, tumor location, and grade of differentiation. Thus, a study exploring the radiologic signature associated with the LN metastasis is urgently needed. In our study, the arterial rad-score was independently and positively associated with the risk of LN metastasis both as a continuous variable and a categorical variable ($P < 0.05$).

At present, there are only a few studies that have predicted LN metastasis using radiomics. Wu et al[11] and Ji et al[15] developed and validated a radiomics nomogram that incorporated the radiomics signature and CT-reported LN status. They showed good calibration and discrimination in training and validation sets in cases with colorectal cancer and biliary tract cancer, respectively. Huang et al[13] also developed and validated a radiomics nomogram that included the radiomics signature, carcinoembryonic antigen level, and CT-reported LN status; the prediction model yielded a C-index of 0.736 (95% CI, 0.730–0.742) in a training set and 0.778 (95% CI, 0.769–0.787) in a validation set. Although these studies developed a prediction model, the exact relationship between the rad-score and the LN metastasis remained unknown. In the current study, we found that the arterial rad-score and the T stage are independently and positively associated with the risk of LN metastasis ($P < 0.05$) by univariate analysis. Moreover, the stratified analysis showed that the impact of the arterial rad-score on LN metastasis was not affected by age, sex, BMI, CA 19-9 level, tumor location, T stage, or grade of differentiation (*P* for interaction <0.05). A significant association between the arterial rad-score and LN metastasis ($P < 0.0001$; OR, 1.43; 95% CI, 1.23–1.66) was found by a model adjusted for age, sex, BMI, CA 19-9, location, T stage, or grade of differentiation on multivariate analyses. Thus, a higher arterial rad-score was associated with a higher risk of LN metastasis (*P* for trend <0.001).

Our study has some limitations. First, this study was retrospective in nature. Second, the possibility of LN micrometastasis in patients with node-negative disease cannot be excluded. Third, the CT-reported LN status was not treated as a covariate, as it is difficult to establish one-to-one correlation between the LN imaging findings and the pathological evidence of LN metastasis.

Thus, in the future, we will combine the rad-score with clinical, pathologic, and genetic features to develop a prediction model. Furthermore, a multicenter study with a larger sample size is needed to acquire high-level evidence for the clinical application of the arterial rad-score.

In conclusion, the arterial rad-score has significant association with the risk of LN metastasis in PDAC. A higher arterial rad-score is associated with a higher risk for LN metastasis. Thus, radiomics analysis may be a promising noninvasive method for assessment of LN metastasis.

REFERENCES

1. Siegel RL, Miller KD, Jemal A. Cancer statistics, 2018. *CA Cancer J Clin*. 2018;68:7–30.
2. Kamisawa T, Wood LD, Itoi T, et al. Pancreatic cancer. *Lancet*. 2016;388: 73–85.
3. Campbell F, Verbeke CS. *Pathology of the Pancreas: A Practical Approach*. London, UK: Springer; 2013.
4. McDermott S, Thayer SP, Fernandez-Del Castillo C, et al. Accurate prediction of nodal status in preoperative patients with pancreatic ductal adenocarcinoma using next-gen nanoparticle. *Transl Oncol*. 2013;6: 670–675.
5. Matsubayashi H, Matsui T, Yabuuchi Y, et al. Endoscopic ultrasonography guided-fine needle aspiration for the diagnosis of solid pancreaticobiliary lesions: Clinical aspects to improve the diagnosis. *World J Gastroenterol*. 2016;22:628–640.
6. Lee YN, Moon JH, Kim HK, et al. A triple approach for diagnostic assessment of endoscopic ultrasound-guided fine needle aspiration in pancreatic solid masses and lymph nodes. *Dig Dis Sci*. 2014;59: 2286–2293.
7. Wunderbaldinger P. Problems and prospects of modern lymph node imaging. *Eur J Radiol*. 2006;58:325–337.
8. Tseng DS, van Santvoort HC, Fegrachi S, et al. Diagnostic accuracy of CT in assessing extra-regional lymphadenopathy in pancreatic and peri-ampullary cancer: a systematic review and meta-analysis. *Surg Oncol*. 2014;23:229–235.
9. Lambin P, Rios-Velazquez E, Leijenaar R, et al. Radiomics: extracting more information from medical images using advanced feature analysis. *Eur J Cancer*. 2012;48:441–446.
10. Kumar V, Gu Y, Basu S, et al. Radiomics: the process and the challenges. *Magn Reson Imaging*. 2012;30:1234–1248.
11. Wu S, Zheng J, Li Y, et al. A radiomics nomogram for the preoperative prediction of lymph node metastasis in bladder cancer. *Clin Cancer Res*. 2017;23:6904–6911.
12. Zhong Y, Yuan M, Zhang T, et al. Radiomics approach to prediction of occult mediastinal lymph node metastasis of lung adenocarcinoma. *AJR Am J Roentgenol*. 2018;211:109–113.
13. Huang YQ, Liang CH, He L, et al. Development and validation of a radiomics nomogram for preoperative prediction of lymph node metastasis in colorectal cancer. *J Clin Oncol*. 2016;34:2157–2164.
14. Dong Y, Feng Q, Yang W, et al. Preoperative prediction of sentinel lymph node metastasis in breast cancer based on radiomics of T2-weighted fat-suppression and diffusion-weighted MRI. *Eur Radiol*. 2018;28: 582–591.
15. Ji GW, Zhang YD, Zhang H, et al. Biliary tract cancer at CT: a radiomics-based model to predict lymph node metastasis and survival outcomes. *Radiology*. 2019;290:90–98.
16. van Griethuysen JJM, Fedorov A, Parmar C, et al. Computational radiomics system to decode the radiographic phenotype. *Cancer Res*. 2017; 77:e104–e107.
17. Tibshirani R. Regression shrinkage and selection via the lasso: a retrospective. *J R Statist Soc B*. 2011;73:273–282.
18. Amin MB, Edge SB, Greene FL, et al, eds. *AJCC Cancer Staging Manual*. 8th ed. New York, NY: Springer; 2017.
19. Hartwig W, Hackert T, Hinz U, et al. Pancreatic cancer surgery in the new millennium: better prediction of outcome. *Ann Surg*. 2011;254:311–319.
20. Michalski CW, Kleeff J, Wente MN, et al. Systematic review and meta-analysis of standard and extended lymphadenectomy in pancreaticoduodenectomy for pancreatic cancer. *Br J Surg*. 2007;94: 265–273.
21. Iqbal N, Lovegrove RE, Tilney HS, et al. A comparison of pancreaticoduodenectomy with extended pancreaticoduodenectomy: a meta-analysis of 1909 patients. *Eur J Surg Oncol*. 2009;35:79–86.
22. Wallace MB, Kennedy T, Durkalski V, et al. Randomized controlled trial of EUS-guided fine needle aspiration techniques for the detection of malignant lymphadenopathy. *Gastrointest Endosc*. 2001;54:441–447.
23. Yasuda I, Iwashita T, Doi S. Tips for endoscopic ultrasound-guided fine needle aspiration of various pancreatic lesions. *J Hepatobiliary Pancreat Sci*. 2014;21:E29–E33.
24. Hikichi T, Irisawa A, Bhutani MS, et al. Endoscopic ultrasound-guided fine-needle aspiration of solid pancreatic masses with rapid on-site cytological evaluation by endosonographers without attendance of cytopathologists. *J Gastroenterol*. 2009;44:322–328.
25. Varadarajulu S, Bang JY, Holt BA, et al. The 25-gauge EUS-FNA needle: good for on-site but poor for off-site evaluation? Results of a randomized trial. *Gastrointest Endosc*. 2014;80:1056–1063.
26. Itoi T, Tsuchiya T, Itokawa F, et al. Histological diagnosis by EUS-guided fine-needle aspiration biopsy in pancreatic solid masses without on-site cytopathologist: a single-center experience. *Dig Endosc*. 2011;23(Suppl 1): 34–38.
27. Tamm EP, Balachandran A, Bhosale PR, et al. Imaging of pancreatic adenocarcinoma: update on staging/resectability. *Radiol Clin North Am*. 2012;50:407–428.
28. Chang J, Schomer D, Dragovich T. Anatomical, physiological, and molecular imaging for pancreatic cancer: current clinical use and future implications. *Biomed Res Int*. 2015;2015:269641.
29. Fromm H, Rodgers JB Jr. Effect of aminopterin on lipid absorption: depression of lipid-reesterifying enzymes. *Am J Physiol*. 1971;221: 998–1003.
30. Howard TJ, Chin AC, Streib EW, et al. Value of helical computed tomography, angiography, and endoscopic ultrasound in determining resectability of periampullary carcinoma. *Am J Surg*. 1997;174:237–241.
31. Imai H, Doi R, Kanazawa H, et al. Preoperative assessment of para-aortic lymph node metastasis in patients with pancreatic cancer. *Int J Clin Oncol*. 2010;15:294–300.
32. Midwinter MJ, Beveridge CJ, Wilsdon JB, et al. Correlation between spiral computed tomography, endoscopic ultrasonography and findings at operation in pancreatic and ampullary tumours. *Br J Surg*. 1999;86: 189–193.
33. Nanashima A, Tobinaga S, Abo T, et al. Evaluation of surgical resection for pancreatic carcinoma at a Japanese single cancer institute. *Hepatogastroenterology*. 2012;59:911–915.
34. Harisinghani MG, ed. *Atlas of Lymph Node Anatomy*. New York, NY: Springer; 2013.
35. House MG, Gönen M, Jarnagin WR, et al. Prognostic significance of pathologic nodal status in patients with resected pancreatic cancer. *J Gastrointest Surg*. 2007;11:1549–1555.